DRUG DEVELOPMENT AND INDUSTRIAL PHARMACY, 20(7), 1213-1224 (1994)

TRANSPORT OF METHOTREXATE DIALKYL ESTER PRODRUGS ACROSS FULL-THICKNESS HAIRLESS MOUSE SKIN

James J. Fort[1], Zezhi Shao, and Ashim K. Mitra[X]

Department of Industrial and Physical Pharmacy
School of Pharmacy and Pharmacal Sciences
Purdue University
West Lafayette, IN 47907

1. Present address: Abbott Laboratories
Pharmaceutical Products Division
North Chicago, IL 60064

ABSTRACT

The permeability coefficients of methotrexate (MTX) and a series of its mono and dialkyl ester prodrugs across full-thickness hairless mouse skin have been determined using an in vitro diffusion method. MTX was found to permeate across this skin model with a mean permeability of 5.6×10^{-5} cm/hr. Monoesterification only slightly improved MTX permeation and the effect appeared to be invariant with alkyl chain length. Diesterification of MTX, on the other hand, resulted in derivatives prone to simultaneous conversion during permeation by both skin esterase and chemical hydrolysis in the diffusion medium. The contribution of conversion to overall MTX diffusion was treated mathematically in order to calculate the intrinsic permeabilities of MTX dialkyl esters. It was found that the dialkyl esters showed a parabolic permeability versus chain length relationship with the dimethyl ester being the most permeable compound.

[X] To whom all correspondence should be directed

INTRODUCTION

Methotrexate (MTX), an antifolate chemotherapeutic agent has been used for many years in the therapy of various forms of neoplasms including choriocarcinoma and acute lymphoblastic leukemia (1,2). More recently, MTX has been utilized successfully in the treatment of severe and otherwise unresponsive cases of psoriasis (3). This application, however, requires the drug to be administered systemically, thus exposing the patient to all of MTX's potentially dangerous toxicities (4). Attempts to deliver MTX topically to the psoriatic lesions have been less encouraging (5). After extensive investigation it has been determined that the possible reasons of MTX's topical ineffectiveness are its inadequate penetration through the stratum corneum (6), as well as its rapid removal from the viable epidermis, the site of action, via a dermal clearance mechanism (7).

The preparation of linear lipid soluble diester homologs of MTX has been described previously, as has been the study of their hydrophobic parameters as a function of alkyl chain length (8). Reasonable anti-psoriatic activity was noticed in skin plug assays for some of these diesters (9-11). However, a very limited study on their permeability determination through human cadaver skin has been reported (5). This report describes a part of our continued effort in the evaluation of the hairless mouse skin permeability and the extent of chemical and enzymatic conversion of a homologous series of MTX dialkyl esters. Skin permeabilities were also calculated for MTX monoalkyl esters.

MATERIALS AND METHODS

MATERIALS

MTX was generously donated by American Cyanamid Co., Pearl River, New York. The preparation of some of the compounds used in this study, namely dimethyl MTX (DMMTX), diethyl MTX (DEMTX), dipropyl MTX (DPMTX), and diisopropyl MTX (DIPMTX), have been described previously (8,12,13). The isomeric monoalkyl MTX mixtures, namely α- and γ-isomers of methyl (MMTX), ethyl (EMTX), propyl (PMTX), and isopropyl (IPMTX), were synthesized by a slight modification of the method of Rosowsky et al. (14). The preparation of individual monoester reference samples of α-EMTX, γ-EMTX, α-PMTX, γ-PMTX, α-IPMTX, and γ-IPMTX were described elsewhere (15). Chemical structures of the compounds utilized in this study are shown in Scheme I.

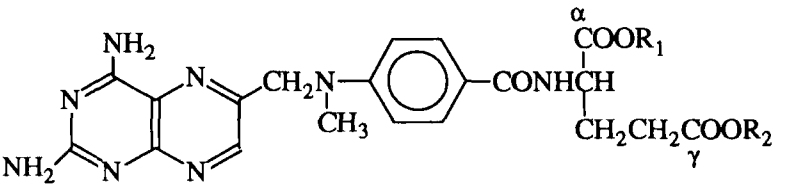

Scheme I

Compound	R_1	R_2
Methotrexate (MTX)	H	H
Dimethyl Methotrexate (DMMTX)	CH_3	CH_3
Diethyl Methotrexate (DEMTX)	CH_2CH_3	CH_2CH_3
Dipropyl Methotrexate (DPMTX)	$CH_2CH_2CH_3$	$CH_2CH_2CH_3$
Diisopropyl Methotrexate (DIPMTX)	$CH(CH_3)_2$	$CH(CH_3)_2$
α-Methyl Methotrexate (α-MMTX)	CH_3	H
γ-Methyl Methotrexate (γ-MMTX)	H	CH_3
α-Ethyl Methotrexate (α-EMTX)	CH_2CH_3	H
γ-Ethyl Methotrexate (γ-EMTX)	H	CH_2CH_3
α-Propyl Methotrexate (α-PMTX)	$CH_2CH_2CH_3$	H
γ-Propyl Methotrexate (γ-PMTX)	H	$CH_2CH_2CH_3$
α-Isopropyl Methotrexate (α-IPMTX)	$CH(CH_3)_2$	H
γ-Isopropyl Methotrexate (γ-IPMTX)	H	$CH(CH_3)_2$

METHODS

HPLC Analysis of MTX and Its Ester Derivatives

HPLC analyses of the dialkyl esters of MTX were carried out with pH 3 (0.05 M KH_2PO_4)/acetonitrile (ACN) mobile phases varying from 72.5/27.5 to 55/45 (V/V) proportions, and containing 5 mM triethanolamine (TEA). The stationary phase consisted of a 15 cm Novapak C-18 column (Waters Associates). Flow Rates were kept constant at 1.0 ml/min. Monoester and MTX assays, except for MMTX required pH 7 (0.002 M KH_2PO_4)/methanol (MeOH) mobile phases varying from 65/35 to 55/45 (V/V) proportions containing 5 mM tetrabutyl ammonium phosphate (TBAP). The analysis utilized a 15 cm Resolve C-18 column (Waters). α- and γ-MMTX isomers were separated with 72.5/27.5 (V/V) proportions of the above mobile phase on a 25 cm Phase-II C-18 column

(Bioanalytical Systems). Flow rates were 1.5 ml/min. The HPLC equipment assembly consisted of a M-6000A pump, 440 single wavelength detector set at 254 nm, a U6K injector (Waters), an Omniscribe B-5000 strip chart recorder (Houston Instruments), and a Chromatopac E-1A integrator (Shimadzu).

Unknown concentrations were determined from standard curves of diesters, monoester mixtures, and MTX.

Transport Studies Across Full-Thickness Hairless Mouse Skin

The diffusion apparatus utilized in all of the skin transport studies has been described in detail previously (16). These cells (DC-100B, Crown Glass) have a 3.4 ml internal volume, and 0.636 cm^2 diffusion area, with built-in water jacketing system for constant temperature. Stirring was accomplished with a magnetic stirrer (Scientific Products), and internally mounted star head magnets. Temperature was maintained with a small volume bath (MGW Lauda), circulating water through the external jacket of the diffusion cells via tygon tubing.

Male hairless mice (HRS/J Strain), 10-13 weeks of age, were sacrificed by cervical dislocation. The skin was removed from the animal by lifting it from underlying fascia. The sample membrane was cleaned with tweezers to remove subcutaneous fat and other tissue debris. Then after dividing it into approximately two equal halves, each section was mounted between the diffusion cells. Diffusion medium was added to both donor and receptor sides and allowed to equilibrate with the skin at 37 °C for 24 hours with constant stirring. Following that period, the diffusion medium was removed from the donor and receptor cells. Each cell was rinsed once with the fresh diffusion medium. Fresh medium was then added to the receptor side. A saturated solution of the diester or MTX containing excess solid, or 2.8 mM monoester pair mixtures (γ/α=3:1, ref. 17)was added to the donor side. Then at 12 hour time intervals for 96 hours, samples were withdrawn from the donor and receptor phases and frozen until analysis. In the case of the receptor, the volume removed (2×50 µl) was replaced by fresh diffusion medium. No replacement was necessary on the donor side. The receptor compartment was analyzed for diester, monoester, and MTX while the donor was analyzed for monoester and MTX by the HPLC methods described previously.

RESULTS AND DISCUSSION

The chemical structures of MTX, its monoalkyl ester derivatives, and its dialkyl ester prodrugs have been illustrated in Scheme I. The synthetic pathways,

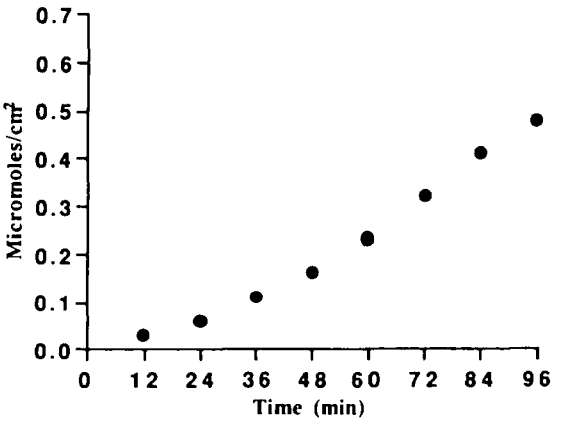

FIGURE 1
Appearance of total drug in the receptor following permeation of DMMTX across full-thickness hairless mouse skin .

physicochemical properties, chromatographic characterization, stability in aqueous media, and transport and bioconversion characteristics across tape-stripped hairless mouse skin have all been reported previously from this laboratory (8,15-17). We have continued this investigation by further characterizing their transdermal permeabilities through the full-thickness skin model.

In most cases, permeation across full-thickness skin is essentially controlled by the outermost stratum corneum layer, the principle rate limiting barrier to relatively hydrophilic molecules across the skin (18). Due to the slow penetration process, this study was undertaken over a period of 96 hours with every 12 hour sampling. Before the initiation of a diffusion experiment, the skin sample was allowed to equilibrate with the diffusion medium for 24 hours prior to the experiment. After this equilibration period, the donor diffusion cell was filled with a saturated solution of the diester.

The HPLC chromatograms revealed the appearance of both the intact diester and hydrolyzed isomeric monoester pairs in the receptor cell during the transport experiment. A representative plot of the total appearance of all species (diester and monoesters) in the receptor phase has been illustrated in Figure 1 for the permeation of DMMTX. The total amount transported against time plot

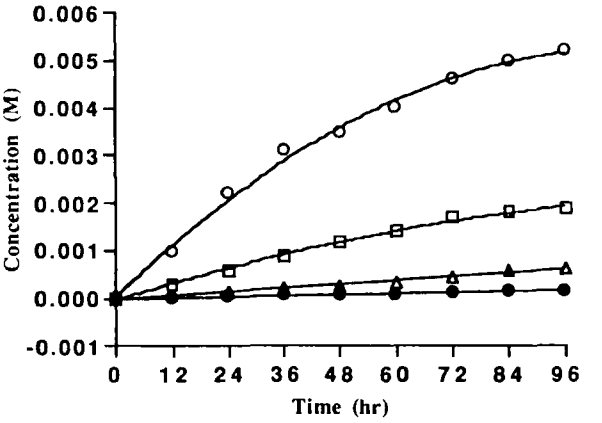

FIGURE 2

Donor appearance of MMTX (○), EMTX (□), PMTX (Δ), and IPMTX (●) during diffusion through full-thickness hairless mouse skin. Values represent the means of 4-8 determinations.

exhibits an upward curvature indicating the contribution of additional amount of hydrolytic species in the receptor phase in addition to what would be observed from the diester gradient alone. Over the course of an experiment i.e., 96 hours, monoesters may have been formed in the donor solution due to chemical hydrolysis and then diffuse across the membrane. Any flux due to monoesters formed in this manner must be subtracted from the total flux since this transport is not related to the inherent flux of the diester.

HPLC assay of the donor compartment samples indeed confirmed that accumulation of monoesters during the permeation process. The accumulation profiles (Figure 2) appear to follow asymptotic to linear lines. These lines have been best fitted by nonlinear equations as compiled in Table 1.

The contribution of monoester flux to the overall pattern for the diesters may be assessed by determining monoester permeability separately. Therefore each of the monoester mixtures, i.e., MMTX, EMTX, PMTX, and IPMTX was studied for its permeability across full-thickness hairless mouse skin. Donor concentrations of alpha/gamma monoester pair mixtures (1:3) of 2.8 mM were used and studies were conducted for 96 hours. The observed monoester steady-state fluxes and permeabilities are summarized in Table 2 while a representative

TABLE 1
Empirical Equations Describing Monoester Formation in Donor Cell following Permeation Experiments of MTX Dialkyl Esters across Full-Thickness Hairless Mouse Skin

Dialkyl Ester	Empirical Equation*	Goodness of Fit (r)
DMMTX	$C(t) = 2.82\times10^{-4} + 8.35\times10^{-5}t - 3.03\times10^{-7}t^2$	0.992
DEMTX	$C(t) = 2.69\times10^{-5} + 2.82\times10^{-5}t - 9.82\times10^{-8}t^2$	0.999
DPMTX	$C(t) = -2.46\times10^{-5} + 6.68\times10^{-6}t$	0.990
DIPMTX	$C(t) = 9.80\times10^{-6} + 1.35\times10^{-6}t$	0.988

* t in hours and C(t) in moles/liter

TABLE 2
Observed Monoester Steady-State Fluxes and Permeabilities Through Full-Thickness Hairless Mouse Skin (n=3-6)

Compound	Mean Steady-State Flux (μmoles/cm^2/hr)	Permeability (cm/hr) (mean±SD)
MTX	4.012×10^{-4}	$5.644\times10^{-5}\pm3.357\times10^{-5}$
MMTX	2.674×10^{-4}	$1.039\times10^{-4}\pm1.470\times10^{-5}$
EMTX	2.075×10^{-4}	$7.655\times10^{-5}\pm2.130\times10^{-5}$
PMTX	2.497×10^{-4}	$9.306\times10^{-5}\pm1.076\times10^{-5}$
IPMTX	3.125×10^{-4}	$1.106\times10^{-4}\pm3.556\times10^{-5}$

flux diagram is shown in Figure 3. Compared to MTX, the permeability of the monoesters increased only slightly. There was no apparent dependence of permeability on chain length.

Once the formation rate of monoesters and their permeabilities have been determined it is fairly simple to calculate the rate of appearance of the monoester in the receptor as a function of time according to the following equations:

$$\text{Receptor Flux} = \frac{dA}{dt} = P^*C(t) \quad (1)$$

$$dA = P * C(t)^*dt \quad (2)$$

$$\int_{A(0)}^{A(t)} dA = P^* \int_{t=0}^{t} C(t)dt \quad (3)$$

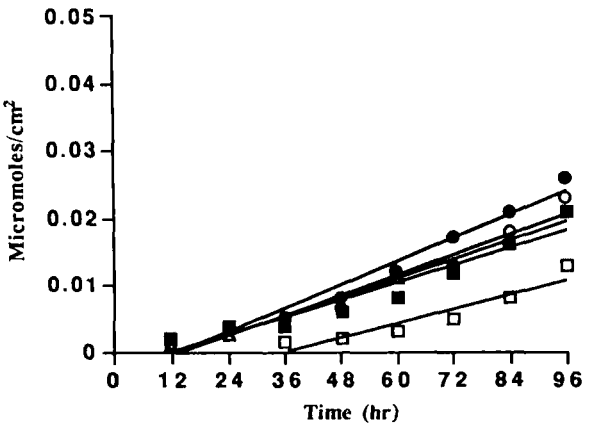

FIGURE 3

Receptor appearance of MMTX (○), EMTX (□), PMTX (Δ), and IPMTX (●) after diffusion through full-thickness hairless mouse skin. Values represent the means of 3-6 determinations. Error bars not shown for clarity.

where A is the amount of monoester transported (μmoles/cm^2), at time t (hr). P is the monoester permeability (cm/hr), and C(t) represents the monoester concentration (in moles/L) generated in the donor cell during diffusion (Table 1). When this equation is integrated, an expression for the amount of monoester in the receptor at time t can be obtained. An example of an integrated expression is shown in Eq. 4 for the appearance of monomethyl MTX in the receptor of a full-thickness skin experiment as a function of time.

$$A(t)=1000(1.04\times10^{-4})[2.82\times10^{-4}t + 8.35\times10^{-5}\frac{t^2}{2} - 3.03\times10^{-7}\frac{t^3}{3}] \quad (4)$$

When similar expressions are generated for each monoester pair, analogous receptor flux curves due to monoester diffusion result. When these monoester fluxes are subtracted from the overall observed total flux curves, the resulting fluxes from donor diester only are obtained. These plots are shown in Figure 4 and such corrected steady-state fluxes have been summarized in Table 3.

For easy comparison, the permeabilities of the diesters, monoesters and MTX across full-thickness hairless mouse skin are all listed in Tables 2 & 3. In

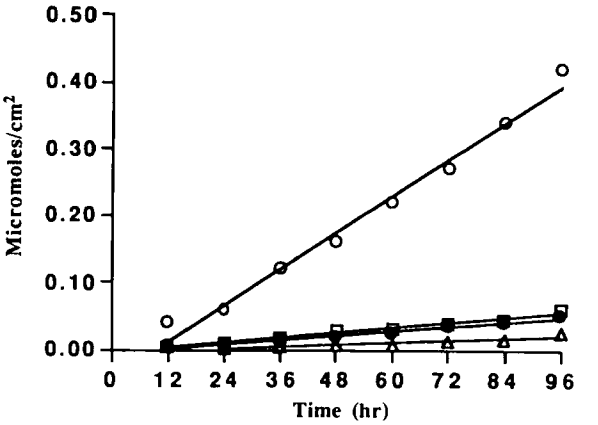

FIGURE 4
Receptor appearance of total drug due to DMMTX (○), DEMTX (□), DPMTX (Δ), and DIPMTX (●) following diffusion through full-thickness hairless mouse skin. Values represent the means of 4-8 determinations. Error bars not shown for clarity.

TABLE 3
Full-Thickness Skin Permeabilities for MTX and Its Dialkyl Esters

Compound	Steady-State Flux (μmoles/cm^2/hr)	Permeability (cm/hr) (mean±SD)	n
MTX	4.012×10^{-4}	$5.644\times10^{-5}\pm3.357\times10^{-5}$	6
DMMTX	5.145×10^{-3}	$5.955\times10^{-4}\pm2.941\times10^{-4}$	8
DEMTX	7.724×10^{-4}	$1.527\times10^{-4}\pm7.394\times10^{-5}$	8
DPMTX	3.254×10^{-4}	$1.162\times10^{-4}\pm9.062\times10^{-5}$	4
DIPMTX	5.405×10^{-4}	$1.290\times10^{-4}\pm5.195\times10^{-5}$	4

the monoester series, the permeability improvement over MTX is slight, with no apparent relationship to chain length. The diesters on the other hand exhibit a parabolic type relationship between permeability and chain length. From MTX to DMMTX, there is a 10 fold increase in permeability. But as the series is ascended, there is a substantial drop in permeability, although DEMTX, DPMTX, and DIPMTX still exhibit a 2 to 3 fold increase in permeability as compared to MTX.

The interpretation of this data requires consideration of the structure of the full-thickness mouse skin, and the various pathways involved in drug transport through such a membrane, particularly through the stratum corneum. It is a highly complex layer composed of keratinized cells tightly opposed to one another. Between cells is alternating layers of lipid and water (19). Under experimental conditions, the stratum corneum is highly solvated with the transport medium. As a result a series of layers of keratinized cells are dispersed in a highly solvated, relatively polar environment. Therefore, a diffusing molecule is required to possess good biphasic affinity, in that not only must it have a lipophilic component to its structure, but also must maintain good polar (solvent) affinity. Considering the partition coefficient data and solubility data in the diffusion medium (8,17), the dimethyl ester achieves both an increase in lipophilicity, and an increase in solubility relative to MTX. Further increases in the chain length of this homologous series exhibit a further increase in lipophilicity, accompanied by a sharp decline in diffusion medium solubility. Therefore, the compounds are developing progressively lower affinity for the biophase medium.

Since MTX being a dianionic glutamate at physiologic pH is not considered a highly lipophilic molecule, previous studies on its skin permeability revealed that the mechanism of transport across the stratum corneum is primarily through the appendageal pathway, with a small component due to transcellular (lipoidal) permeation (20). When the dianionic character of MTX is modified by esterification to form the dimethyl ester, there is a considerable increase in the compound's ability to traverse the transcellular pathway. Simultaneously, however, the molecule will encounter a heavily solvated environment between the lipoidal layers, as well as within the parallel appendageal pathway. DMMTX still retains good affinity for this polar solvated part of the stratum corneum environment.

Higher lipophilic members of the series may possess the lipophilicity necessary to permeate the lipoidal transcellular components of the membrane, but become limited by the parallel appendageal route as well as by the intercellular solvated environment.

A similar phenomenon was observed with the stripped skin studies where DMMTX shows a significant improvement in permeability over MTX but higher chain length members of the series show a progressive decline in permeability

(16). The effect is however more pronounced with the full-thickness skin study. This is not entirely surprising since the stratum corneum is a more substantial barrier, and may exhibit effects similar to the viable epidermal layer of the stripped skin, although to a larger extent.

The biphasic affinity discussed previously is the major factor in the permeability profile seen in stripped and full-thickness skin studies. Their effects are qualitatively the same in both types of membranes, although they differ in magnitude. A quick examination of the stripped and full-thickness permeability data may indicate that because both membranes contain the viable epidermis and dermis layers, it is one or both of those layers responsible for the parabolic permeability vs. chain length relationship. Such a conclusion would be erroneous since, by inspecting the permeability ratio of stripped skin to full-thickness skin a 100 to 1000 fold difference is observed. Thus, although the phenomena seen in the full-thickness and stripped layers are largely dependent on biphasic affinity, the effects are isolated to the stratum corneum and viable epidermis, respectively.

ACKNOWLEDGMENTS

The authors wish to thank Lederle Laboratories for their financial support during this project. J.J.F is also an American Foundation for Pharmaceutical Education Fellow. Instrumentation support was provided in part by NIH Biomedical Research Support Grant RR 05586 and in part by NIH grant NS 25284

REFERENCES

1. S. Farber, L.K. Diamond, R.D. Mercer, R.F. Sylvester, and V.A. Wolff, N. Engl. J. Med., 238, 787 (1948).
2. B.A. Kamen, in "Metabolism and Action of Anti-cancer Drugs", G. Powis and R.A. Prough, eds., Taylor and Francis, London, 1987, pp. 141.
3. G.D. Weinstein and P. Frost, Arch. Dermatol., 103, 33 (1971).
4. G.D. Weinstein, Ann. Intern. Med., 86, 199 (1977).
5. J.L. McCullough, D.S. Snyder, G.D. Weinstein, A. Friedland, and B. Stein, J. Invest. Dermatol., 66, 103 (1976).
6. S.M. Wallace, J.O. Runikis, and W.D. Stewart, Can. J. Pharm. Sci., 13, 66 (1978).
7. O. Siddiqui, M.S. Roberts, and A.E. Polack, Int. J. Pharm., 27, 193 (1985).

8. J.J. Fort and A.K. Mitra, Int. J. Pharm., 36, 7 (1987).
9. J.L. McCullough and G.D. Weinstein, J. Invest. Dermatol., 63, 464 (1974).
10. G.D. Weinstein and J.L. McCullough, Arch. Dermatol., 111, 471 (1975).
11. J.L. McCullough, G.D. Weinstein, and J.B. Hynes, J. Invest. Dermatol., 68, 362 (1977).
12. D.G. Johns, D. Farquhar, M.K. Wolpert, B.A. Chabner, and T.L. Loo, Drug Metab. Disp., 1, 580 (1973).
13. A. Rosowsky, J. Med. Chem., 16, 1190 (1973).
14. A. Rosowsky, G.P. Beardsley, W.D. Ensminger, H. Lazarus, and C. -S. Yu, J. Med. Chem., 21, 380 (1978).
15. J.J. Fort and A.K. Mitra, Org. Proc. Prep Int., (1993) Submitted.
16. J.J. Fort, Z. Shao, and A.K. Mitra, Int. J. Pharm., (1993) In Press.
17. J.J. Fort and A.K. Mitra, Int. J. Pharm., 59, 271 (1990).
18. R.J. Scheuplein and I.H. Blank, Physiol. Rev., 51, 702 (1971).
19. B.W. Barry, J. Control. Rel., 6 85 (1987).
20. S.M. Wallace and G. Barnett, J. Pharm. Biopharm., 6, 315 (1978).